Photonuclear magnetism of silicon in weak magnetic fields

L. S. Vlasenko, N. V. Zavaritskiĭ, S. V. Sorokin, and V. G. Fleĭsher

Institute of Physics Problems, USSR Academy of Sciences, and A. F. Ioffe Physicotechnical Institute, USSR Academy of Sciences
(Submitted 2 April 1986)
Zh. Eksp. Teor. Fiz. **91**, 1496–1508 (October 1986)

A magnetically dilute Si^{29} spin system in a silicon lattice is investigated in weak magnetic fields under conditions of high photonuclear magnetic susceptibility, which is achieved by optical cooling of the spin system to 10^{-4}–10^{-5} K. The resonance responses of the Si^{29} nuclei are recorded at 4.2 K with a SQUID. The "heating" spectra in constant fields B_0 of the order of the local nuclear field B_L are investigated by measuring the rates of magnetization relaxation by alternating fields of various frequencies. These spectra include intense two- and three-spin transitions. Under conditions $B_0 > B_L$, reversal of magnetization is observed on passing through two-spin resonances. The change of the longitudinal magnetization in adiabatic fast passage of the resonances corresponds in a rotating coordinate frame to a local field B'_L = (0.06 ± 0.02) G. Standard NMR technique is used to find the true width δ of the NMR lines [the maximum-slope points yield δ = (0.12 ± 0.02) G], and lines corresponding to transitions between triplet states of pairs of nuclei located in nearest lattice sites are observed. The effect of relaxation on the photoinduced paramagnetic centers is investigated. The effectiveness of SQUID for the study of photonuclear magnetism is compared with that of NMR.

1. INTRODUCTION

Optical orientation of electron spins in interband absorption of light in semiconductors is known to be able to cool effectively the spin system of the lattice nuclei.[1-4] The increase of nuclear magnetic susceptibility χ_0 by this cooling of the nuclear spin system is the basis of photonuclear magnetism. The susceptibility increment χ_{0C} due to the action of the light can exceed by several orders of magnitude the value of χ_{0T} corresponding to thermodynamic equilibrium at the lattice temperature ($\chi_0 = \chi_{0C} + \chi_{0T}$). This uncovers new possibilities of investigating nuclear systems in weak magnetic field.

Photonuclear magnetism in weak magnetic fields was investigated until recently mainly by optical methods.[2-6] Information on the nuclear spin system could be obtained only indirectly from the value of the nuclear effective magnetic field due to hyperfine interaction and influencing the polarization of the electron spin system. Nuclear magnetization produced by light in a semiconductor was first measured directly in silicon by a standard NMR technique.[7] The long spin-lattice relaxation time of the Si^{29} nuclei has made it possible to determine the mechanism of their optical polarization in weak magnetic fields by subsequently measuring the magnetization in the strong field of an NMR microwave spectrometer.[8,9]

The behavior of nuclear spin systems of a solid in a weak magnetic field can be studied directly using the superconducting quantum magnetometer of a SQUID.[10] This uncovers new possibilities, compared with the standard NMR procedure, of studying photonuclear magnetism. Thus, it is easy to measure the longitudinal component of the magneti-

zation with the aid of a weak alternating field (or even in the absence of such a field, if the sample is moved), whereas in the standard NMR technique the magnetization is determined by measuring the transverse component in adiabatic fast passage through resonance in a strong alternating field.

The possibility of measuring the longitudinal magnetization is also a promising method of finding the nuclear-spin-system magnetic ordering that can result from optical cooling.[11] The use of a SQUID to investigate photonuclear magnetism permits a study of the dynamics of the processes in a nuclear spin system in a weak field, as well as of the effects due to the nonsecular part of the Hamiltonian that describes this dynamics.

We report here the results, obtained mainly with a SQUID, of an investigation of photonuclear magnetism in a magnetically dilute system of a silicon-lattice nuclei.

2. EXPERIMENTAL PROCEDURE

The object chosen for the study of photonuclear magnetism was single-crystal silicon containing radiation defects. An important role in the onset of photonuclear magnetism is played by the presence of lattice defects with broken bonds, which can capture photoexcited electrons under conditions of optical irradiation. The electron spectrum of these defects contains triplet states whose magnetic sublevels can have a population different from the equilibrium value even when illuminated by unpolarized light.[12]

Hyperfine interaction of lattice nuclei with an electron system that is not in spin equilibrium is accompanied by dynamic cooling of the ensemble of nuclear spins. The maximum cooling of the nuclear spin system is reached at exter-
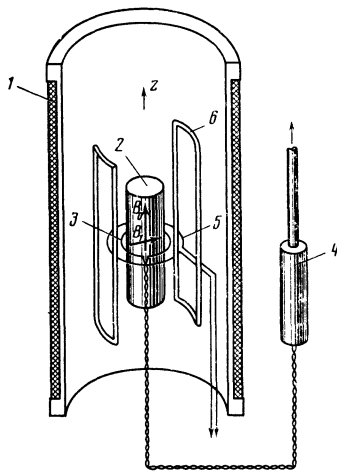
FIG. 1. Experimental setup: 1—solenoid, 2—sample, 3—loop for coupling to SQUID, 4—SQUID, 5—calibrating turn, 6—alternating-field excitation windings.

nal magnetic field values corresponding to anticrossing of the magnetic sublevels of the triplet centers. For most triplet centers in silicon, these magnetic fields lie in the range 20–500 G (Ref. 12). Moving the irradiated crystal into the weaker measuring field of a helium creostat is accompanied by additional lowering of the spin temperature.

By varying the density of the radiation defects it is possible to select samples with optimal spin-lattice relaxation time T_1. This time should be long enough to permit moving the sample to the measuring cryostat and subsequent measurements without noticeable heating of the spin system via spin-lattice relaxation. On the other hand, the illumination time T_1 must not be too long, so that the illumination-measurement cycles can be repeated frequently enough.

In the present study we used pure silicon single crystals irradiated with neutrons at a dose $\approx 2 \cdot 10^{17}$ cm^{-2}. The illumination time T_1 of these samples was ≈ 30 min.

The illumination was carried out in a 300 G field at 77 K, using polarized light from two 500-W incandescent lamps placed on opposite sides of the sample. The samples were cylinders of 6 mm diameter and 10 mm height, with the cylinder axis along the $\langle 111 \rangle$ axis of the crystal. After 30 minutes of illumination, the sample was transferred to the cryostat with the SQUID. The setup is illustrated in Fig. 1. The constant magnetic field was produced with a short-circuited superconducting solenoid. The Earth's field was lowered to $\approx 5 \cdot 10^{-2}$ G by an outer Permalloy shield. Sample 2, mounted on a rod, was inserted through the port of the cryostat, along the solenoid axis, to the interior of the superconducting-transformer loop 3 that ensured magnetic coupling with the SQUID 4 (Ref. 13). This loop, of 1 cm diameter, was placed in a plane perpendicular to the solenoid and passing through its center. Located in the same plane was a calibrating loop 5 of 8 mm diameter, coaxial with loop 3. The sensitivity of the apparatus was calibrated against the magnetic moment of the current flowing though this turn. The nuclear magnetic resonance was excited by an oscillating

field $2B_1 \cos \omega t$ perpendicular to B_0. This field was produced by a pair of rectangular loop windings 6.

The influence of the alternating field on the SQUID operation was reduced by placing the coupling loop 3 in an annular shield. The entire setup was placed in superconducting lead shield.

3. EXPERIMENTAL RESULTS AND DISCUSSION
3.1 Measurement of nuclear magnetization with a SQUID

The photonuclear magnetic susceptibility can be determined by using a SQUID to measure the magnetic moment M produced in a unit volume of the sample in the field B_0 of the solenoid. This measurement can be implemented either by moving the sample along the solenoid axis through loop 3, or by turning on an alternating field B_1 under NMR conditions. In the latter case the sample is kept immobile inside the coupling loop and the change of the magnetic flux through this loop is measured either by reversing the magnetization or by relaxing it via "heating" the nuclear spin system by the alternating field. The results that follow were obtained under NMR conditions.

We consider first adiabatic fast passage through resonance, which permits the longitudinal magnetization M_z to be reversed, and thus produces a signal equal to double the magnetization value (disregarding the loss to nonadiabaticity).

Figure 2a shows the frequency dependences of the signal when the frequency $\nu = \omega/2\pi$ of an alternating field of
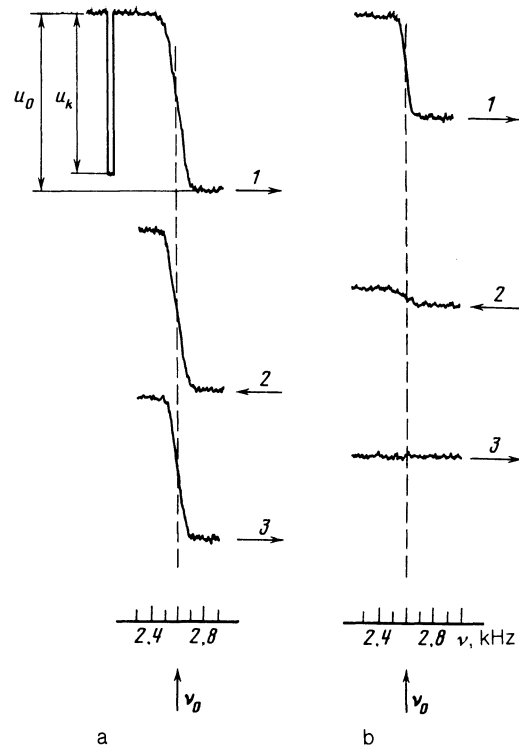

FIG. 2. Variation of longitudinal magnetization M of sample in successive passages (1,2,3) through resonance: a) adiabatic fast passage at $B_1 = 3 \cdot 10^{-3}$ G and $d\nu/dt = 1$ Hz/s; b) diabatic fast passage at $B_1 = 10^{-3}$ G and $d\nu/dt = 10$ Hz/s.

amplitude $B_1 = 4 \times 10^{-3}$ G is scanned near the Larmor frequency $v_0 = \gamma B_0/2\pi$ at a rate $dv/dt = 1$ GHz·s⁻¹ ($\gamma/2\pi = 846$ Hz/G). The solenoid field was 3 G. This scanning rate satisfies the condition for adiabatic fast passage

$$2\pi dv/dt \ll \gamma B_1^2. \tag{1}$$

To determine the resultant magnetization decrease δM_z due to incomplete adiabaticity of the passage through resonance, it is convenient to use the equation obtained by Dzheparov and Fel'dman[14]:

$$\delta M_z = -\frac{1}{6\ln(1/\varepsilon)} - 4.6\varepsilon. \tag{2}$$

The nonadiabaticity parameter here is $\varepsilon = \Delta/\pi(\gamma B_1)^2$, where $\Delta = 2\pi dv/dt$. This equation is valid at the small values of ε realized in the experiment. For $dv/dt = 1$ Hz/s and $B_1 = 3\cdot10^{-3}$ we obtain from (2) $\delta M_z \approx 10\%$.

The dependence of M_z on the frequency ω can then be approximately described by the expression

$$M_z = M_0 \frac{\omega - \omega_0}{[(\omega-\omega_0)^2 + (\gamma B_1)^2 + (\gamma B_L')^2]^{1/2}}; \tag{3}$$

where M_0 is the initial magnetization prior to passage through resonance, and B_L' is the local field of the Si²⁹ nuclei in the rotating coordinate frame.

It can be seen from (2) that when the frequency changes from $\omega < \omega_0$ to $\omega > \omega_0$ the sign of M_z is reversed. The magnetization is reversed after each repeated passage through resonance (see curves 1, 2, and 3 of Fig. 2a).

The plot of the SQUID signal u_0, which is proportional to M_z, vs frequency in Fig. 2a is well described by Eq. (2). Reduction of the experimental $u_0(v)$ curves obtained at different B_1 satisfying condition (1) yields $B_L' = (0.06 \pm 0.02)$ G. When the parameter ε is increased after one passage through resonance, the entropy of the spin system of the Si²⁹ nuclei is noticeably increased, as is also its spin temperature. This "heating" can be accompanied by total loss of the magnetization and takes place both when the frequency sweep is increased and when the field B_1 is decreased. For example, on going through resonance at a rate 10 Hz/s in a field $B_1 = 10^{-3}$ G, the value of M decreases steeply and no change of flux is observed already in the third passage through resonance, i.e., the magnetization is "erased" at these values of dv/dt and B_1 (see Fig. 2b). Thus, the value of M_z can be determined both in the adiabatic fast passage regime and in the "erasure" regime.

To this end it is necessary to take also into account the real shape of the sample and to calibrate the SQUID using the known magnetic moment of the calibrating current-carrying coil. The unknown moment per unit sample volume can then be obtained from the relation

$$M_0 = (\xi_k/\xi_0)(u_0/u_k)M_k, \tag{4}$$

where ξ_0 and ξ_k are coefficients determined from the geometry of the samples and of the turns, and relate the magnetic flux through the coupling loop 3 to the measured magnetic moment ($\Phi_{0,k} = \xi_{0,k} \cdot 4\pi M_{0,k}$) for the calibration loop and for the sample, respectively; u_0 and u_k are the SQUID output signals from the sample and from the calibrating current-carrying turn. For the foregoing geometric dimensions of the sample and of loops 3 and 5 we get, using Eq. (A2), $\xi_0 = 0.208$ and $\xi_k = 1.145$. Thus, $M_0 = 5.505 M_k u_0/u_k$.

The change of u_k shown in Fig. 2a corresponds to a calibration magnetic moment of the current $i_k = 1.4\,\mu$A in loop 5. We then find with the aid of (3) that $M_0 = 2.3\cdot10^{-7}$ CGS.

Thus, using a SQUID and one NMR adiabatic fast passage experiment yields the local fields B_L' as well as the magnetization M_0 due to the photonuclear magnetism.

It must be pointed out here that determination of M_0 and B_L' by the standard NMR technique calls for two substantially different experiments, and B_L' can be estimated only if the photonuclear magnetic susceptibility is high enough, so that the true dipole-dipole NMR line width can be observed. The point is that to record NMR of nuclei having low natural abundance and long spin-lattice relaxation times one usually measures the transverse magnetization. The measurement is carried out also under adiabatic fast passage conditions, but using substantially larger amplitudes of the alternating field B_1 than in the case of a SQUID. This is dictated by the need for satisfying condition (1) in the strong constant field B_0 of the NMR spectrometer and for preventing "loss" of the signal, a loss inevitable if $B_1 < B_L'$. At $B_1 \gg B_L'$, however, the NMR line width is determined solely by the value of B_1. Nonetheless, owing to the large value of χ_{0C} it is possible to observe, with the aid of the standard NMR technique, the undistorted line width of the resonance and to discern its peculiarities due to the disorder of the system of paramagnetic Si²⁹ nuclei.

3.2. NMR spectra of optically polarized silicon

For comparison with the foregoing results, we consider the silicon NMR spectra obtained with a standard NMR spectrometer.

Figure 3a shows the usual NMR adiabatic fast passage signal corresponding to thermodynamic equilibrium of a nuclear spin system at room temperature in a field $B_0 = 7$ kG. The signal was obtained at $B_1 \approx 1$ Hz after keeping the sample in the field B_0 for 3 hours to achieve equilibrium polarization. The signal was recorded at a frequency $v_0 = 6.000$ MHz. Since the nuclear magnetization was directed along the effective field under conditions of adiabatic fast passage, the constant field B_0 was modulated (at 15 Hz frequency) and the dispersion signal was recorded.

Figure 3b shows the NMR signal obtained under the same conditions of passage through resonance, but now after illuminating the sample for 30 minutes in a field 250 G. The signal amplitude was increased by a factor ~ 300, and the line width is given as before by the value of B_1.

To observe the undistorted NMR line width it is necessary to satisfy the unsaturated-passage condition:

$$(\gamma B_1)^2 T_1 T_2 \ll 1 \tag{5}$$

and the fast-passage condition that excludes mixing of the Zeeman and dipole-dipole reservoirs:

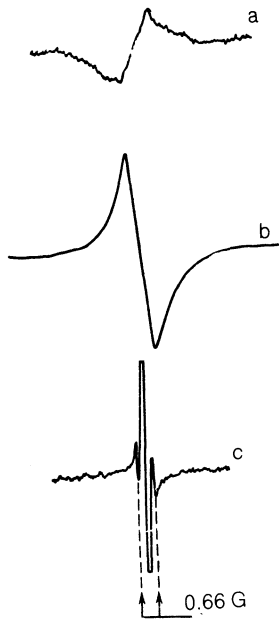$$dB_0/dt \gg \gamma B_1^2. \tag{6}$$

FIG. 3. NMR spectra of silicon: a) adiabatic fast passage signal after 3 hours in darkenss in a field 7 kG at room temperature, $B_1 = 1$ G, $\chi_0 = 6.000$ MHz, $dB_0/dt = 5 \cdot 10^{-2}$ G/s; b) adiabatic fast passage signal after 30 minutes of sample illumination in a 250 G field, $B_1 = 1$ G, $v_0 = 6.000$ MHz, $dB_0/dt = 5 \cdot 10^{-2}$ G/s, amplification decreased by 300 times (compared with a); c) derivative of absorption signal in nonsaturating passage through resonance after 30 min of sample illumination in a field 250 G, $B_1 = 10^{-4}$ G, $v_0 = 6.000$ MHz, $dB_0/dt = 5 \cdot 10^{-2}$ G/s; B_0 oriented along the $\langle 100 \rangle$ axis.

For a spin-spin relaxation time $T_2 \approx 10^{-2}$ s and $T_1 \approx 1$ h we obtain from (5) the condition $B_1 < 10^{-1}$ G, which leads to the condition $dB_0/dt \gg 10^{-5}$ [see (6)].

Figure 3c shows the derivative of the absorption signal of Si^{29} nuclei in a silicon crystal after optical polarization of these nuclei. The signal was obtained at $B_1 = 10^{-4}$ G, $dB_0/dt = 5 \cdot 10^{-2}$ G/s, and the field B_0 along the $\langle 110 \rangle$ axis. The NMR line width δ between the maximum-slope points is (0.12 ± 0.02) G. On both sides of the principal line corresponding to the Larmor frequency v_0 of the Si^{29} nuclei one can see low-intensity but well resolved sideband lines. The distance between these lines, 0.66 G, corresponds to the splitting in the spectrum of isolated Si^{29} pairs located in adjacent sites of the lattice and arranged along the $\langle 111 \rangle$ axes of the crystal. The possibility of separating isolated pairs in silicon is due to the small natural abundance of the Si^{29} nuclei (4.7%). The dipole-dipole interaction between the spins of the nuclear pairs, accidentally located in neighboring sites of the lattice, is much larger than the dipole-dipole interaction of each of the spins of this pair with the spins of the remaining nuclei of the crystal.

It can be easily seen that the number of Si^{29} nuclei included among the pairs produced by the nearest neighbors is 9.4% of the total number of Si^{29} nuclei. Resonant transitions between triplet states of isolated pairs should be observed at the frequencies[15]

$$\omega_i = 2\pi v_i = \gamma B_0 \pm {}^3/_4 \gamma^2 \hbar d^{-3} (1 - 3\cos^2\theta_i), \qquad (7)$$

where d is the distance between the nuclei in the pair and θ_i is the angle between the field B_0 and the ith $\langle 111 \rangle$ axis of the crystal. The splitting of the satellite lines on Fig. 3c corresponds to a distance $d = 2.34$ Å between nearest neighboring nuclei in the silicon lattice, $\theta_{1,2} = 90°$, and $\theta_{3,4} = 35°$.

It should be noted that although the large value of χ_{0C} made it possible to find the width δ of the undistorted NMR line, it is impossible to determine independently the value of B'_L from the spectrum of Fig. 3c, since we know no function that approximates the line shape. To determine the second moment of the line and the value of B'_L we must find the true line shape from experiment; this is a problem in itself. From among the results of the standard NMR technique, we single out here only the proof that triplet states exist in the spin-spin interaction spectrum of a magnetically dilute system of Si^{29} nuclei.

3.3 Photonuclear magnetization in weak magnetic fields

We consider now the dependence of the nuclear magnetization, measured with a SQUID, on the conditions prior to the measurement in a weak magnetic field. Since the slow (in the T_2 time scale) transfer of the sample from the field B_i = 300 Hz in which the optical pumping was carried out at 77 K to the field B_0 of the solenoid of the helium cryostat can be regarded as adiabatic, the final spin temperature Θ_f as a function of the temperature Θ_i reached in the field B_i is given by[16]

$$\Theta_f = \Theta_i (B_0^2 + B_L^2)^{1/2}/B_i, \qquad (8)$$

where B_L is the local field of the nuclei in the laboratory frame. In this case

$$M_z = M_i B_0/(B_0^2 + B_L^2)^{1/2}, \qquad (9)$$

where M_i is the magnetization in the field B_i at the temperature Θ_i. It follows from (9) that the variation of $M_z(B_0)$ is determined by the value of the local field B_L.

Experiment, however, has shown that the variation of $M_z B_0$ depends on whether or not the sample was heated to room temperature directly prior to immersion into the liquid helium. Thus, curve 1 of Fig. 4 was obtained after such a heating, while curve 2 corresponds to measurements made directly after a rapid transfer of the sample from the nitrogen dewar into the helium one. The most probable cause of this discrepancy between curves 1 and 2 is the production, under the influence of the light, of additional paramagnetic nuclear-relaxation centers. It is known that if silicon crystals contain radiation defects illumination causes charge exchange of these defects as a result of their capturing photoexcited electrons or holes. A situation can then arise in which defects that are nonmagnetic in the absence of light become paramagnetic when the crystal is illuminated. The onset of photoinduced paramagnetic centers increases the rate of spin-lattice nuclear relaxation. Effects of optical charge exchange in illuminated n-type silicon were investigated in Ref. 17, where it was shown that photoinduced paramagnetic centers can remain in a crystal 30–50 minutes after the light is turned off.
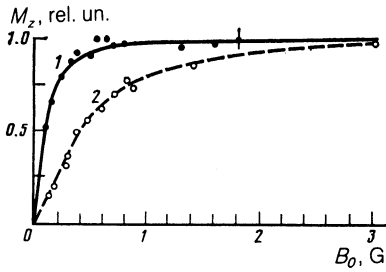
FIG. 4. Magnetization curves $M_z(B_0)$ obtained after annealing the photoinduced paramagnetic centers (1) and without annealing (2). Solid line—calculated from (9) with $B_L = 0.2$ G. The dashed line was drawn for clarity.

To check on the presence of photoinduced paramagnetic centers of the investigated crystals, we investigated their ESR spectra. Figure 5 shows ESR spectra obtained at $T = 77$ K prior to (a) and in the course of (b) illumination under the same conditions as used for optical pumping to investigate photonuclear magnetism. Comparison of spectra (a) and (b) leads to the conclusion that paramagnetic centers are produced in an illuminated crystal at a density $\approx 10^{17}$ cm^{-3} higher by about an order of magnitude than the density of the paramagnetic centers in darkness prior to illumination.

It is known[15] that the rate T_1^{-1} of spin-lattice nuclear relaxation in weak fields is independent of B_0, in view of the difference between the relaxation times T_{1z} and T_{1D} for the Zeeman and dipole reservoirs:

$$T_1^{-1} = T_{1z}^{-1} \frac{B_0^2 + (T_{1z}/T_{1D})B_L^2}{B_0^2 + B_L^2} . \tag{10}$$

For pure dipole-dipole interaction we have $T_{1z}/T_{1D} = 3$. A similar equation determines the field dependence of the rate of nuclear relaxation on photoinduced centers (neglecting the weaker field dependence of the relaxation rate of the centers themselves).

After the light is turned off at 77 K, the density of these centers decreases with a time constant ~ 30 min. If, however, the sample is heated to room temperature immediately after turning off the light, the initial spectrum a of Fig. 5 is restored. Thus, heating the crystals after illumination makes it possible to eliminate the influence of the nuclear spin-lattice relaxation on the photoinduced paramagnetic centers. Curve 1 of Fig. 4 was obtained under these conditions.

The difference between the shapes of curves 1 and 2 in this figure can be characterized by the quantity $\ln(M_{z1}/M_{z2}) \propto T_{1\delta}^{-1}$, where M_{z1} and M_{z2} are the values of the magnetic moments in the field B_0 for curves 1 and 2, respectively, while $T_{1\delta}^{-1}$ is the rate of nuclear relaxation on the photoinduced centers.

Notice must be taken here, however, of the possible influence of the residual (darkness) paramagnetic centers in the sample. They cause apparently some increase of the value $B_L = (0.22 \pm 0.02)$ G determined from the experimental plot of $M_z(B_0)$ (curve 1 of Fig. 4) with the aid of Eq. (9), compared with the calculated value[18] $B_L = 0.176$ G. From the value of M_z at $B_0 = B_L$ we obtain the experimentally

realized maximum photonuclear susceptibility χ_{max} and the minimum spin temperature Θ_{min}. Using the data of Fig. 4 (curve 1) we obtain

$$\chi_{max} = M_z(B_L)/B_L = 8.2 \cdot 10^{-7} \text{ CGS}$$

and

$$\Theta_{min} = N\mu_I^2 I(I+1)/3k\chi_{max} = 1.1 \cdot 10^{-5} \text{ K.}$$

Here $N = 6.53 \cdot 10^{20}$ is the number of Si^{29} nuclei in the sample, μ_I and I are the magnetic moment and the spin of the Si^{29} nucleus, and k is Boltzmann's constant.

The described procedure for optically cooling silicon crystals containing radiation defects has thus made it possible to lower the spin temperature of a system of Si^{29} nuclei by more than 5 orders relative to the lattice temperature of a crystal immersed in liquid helium.

The average spin of the Si^{29} nuclei at Θ_{min} is

$$\langle I \rangle = \mu_I (I+1)B_0/3k\Theta_{min} = 1.8 \cdot 10^{-4}$$

and the degree of orientation is $P = \langle I \rangle/I = 3.6 \cdot 10^{-2}\%$. As the field B_0 is increased, P increases like $B_0/(B_0^2 + B_L^2)^{1/2}$, and reaches $\approx 5 \cdot 10^{-2}\%$ in strong fields ($B_0 \gg B_L$).

3.4. "Heating" of optically cooled nuclear spin system in an alternating magnetic field

One of the interesting consequences of optical cooling of a nuclear system is the possibility of investigating its properties in a field $B_0 \lesssim B_L$. Thus, for example, even at $B_0 = 0$ a cooled spin system should absorb from the alternating field an energy $\langle \hat{B}_1(t)M(t) \rangle$, where $M(t) = \hat{\chi}(v)B_1(t)$ is the nuclear magnetic moment induced by the field $B_1(t)$, and $\hat{\chi}(v)$ is the nuclear susceptibility at the frequency v of the alternating field. In the high-temperature approximation we have $\chi(v) \propto \Theta^{-1}$ and consequently the lower the spin temperature the higher the energy absorbed by the nuclear spin system.

The change of the reciprocal spin temperature $\beta = \Theta^{-1}$ by such "heating" is described by the equation

$$\frac{d\beta}{dt} = -\frac{1}{T_1}(\beta - \beta_0) - \frac{\beta}{T_B}, \tag{11}$$

where T_B^{-1} is the relaxation rate due to absorption of energy
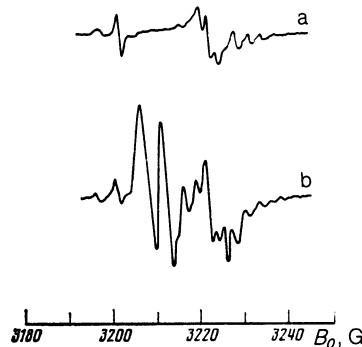

FIG. 5. Variation of ESR spectrum at 77 K and $B_0 \| [111]$ as a result of sample illumination: a) ESR spectrum prior to illumination; b) upon illumination.
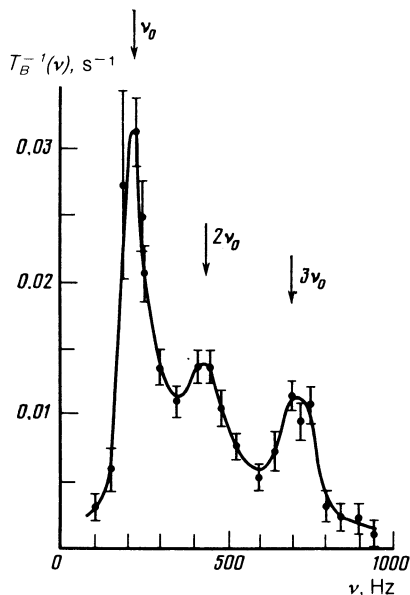
FIG. 6. Spectral dependence of the rate of nuclear relaxation (of the spin-system "heating" under the influence of an alternating field $B_1 = 6 \cdot 10^{-4}$ G in a constant field $B_0 = 0.28$ G.

of the alternating field, and β_0 is the stationary value of β at $B_1 = 0$. In the case considered, $\beta_0 \approx 0$ is the reciprocal temperature of the lattice. Owing to the large value of T_1 it is easy to realize in experiment the condition $T_B \ll T_1$ so that the reciprocal temperature decreases when the alternating field is turned on, from the value $\beta_f = \Theta_f^{-1}$ in acordance with the exponential law $\beta = \beta_f \exp(-t/T_B)$.

If a weak constant field B_0 is turned on to induce in the sample an induced magnetic moment $M_z \propto \beta(t)$, it is possible to investigate, using a SQUID, the dynamics of heating of a nuclear spin system at various frequencies and obtain information on the nuclear-spin correlator corresponding to the total Hamiltonian, including the nonsecular part of the spin-spin interactions.

The frequency dependence of T_B^{-1}, obtained by Merkulov[19] on the basis of the fluctuation-dissipation theorem, is given by

$$T_B^{-1} = \frac{4\pi^2 B_1^2 \nu^2}{(B_0^2 + B_L^2)} \langle \hat{I}_x^2 \rangle_\nu, \qquad (12)$$

where

$$\langle I_x^2 \rangle_\nu = \int_{-\infty}^{\infty} \langle I_x(0) I_x(t) \rangle e^{i2\pi\nu t} \, dt / \mathrm{Sp}(\hat{I}_x^2) \qquad (13)$$

is the Fourier transform of the correlator of the x-component of the average nuclear spin. Here $\hat{I}_x$ is the muclear spin x-projection operator (the field $2B_1\cos\omega t$ is applied along the x axis). Thus, the "heating" spectrum is determined by the frequency dependence of the correlator $\langle I_x^2 \rangle_\nu$ and by the factor ν^2.

The use of a SQUID permits direct determination of the relaxation rates $T_B^{-1}(\nu)$ by measuring the rate of change of M_z following application of an alternating field $B_1(t)$ of fixed frequency ν. Figure 6 shows the results of such mea-

surements, carried out with the aid of a field $B_1 = 6 \cdot 10^{-4}$ G at $B_0 = 0.28$ G. A distinguishing feature of the spectrum in Fig. 6 is the pronounced character of collective (two- and three-spin) processes.

The frequency ν_0 at which the maximum of the intense low-frequency line is observed corresponds to the Larmor frequency of the Si^{29} nuclei in a field B_0, and the second and third maxima correspond to the frequencies $2\nu_0$ and $3\nu_0$ of the two- and three-spin resonances. Attention is called to the fact that the intensities of these lines are comparable. Calculation of the nuclear-spin correlator from the experimental data with the aid of (12) shows that its maximum value near the resonance at the frequency ν_0 is $\approx 0.4 \cdot 10^{-2}$ s. The form of this correlator cannot be approximated by either a Lorentz or a Gauss curve.

As already noted [see Fig. 3c and Eq. (7)], in a magnetically dilute system of silicon nuclei one can separate pairs of nuclei located in neighboring lattice sites with a distance $d = 2.34$ Å between them. These pairs correspond to triplet states with energy levels ε_i, whose position is determined by solving the secular equation $\varepsilon(B_d + \varepsilon) - B_0^2(\varepsilon + B_d\sin^2\theta_i)$, where $B_d = 3\mu_I/2d^3 = 0.656$ G. The corresponding frequencies of the resonant transitions between triplet levels of differently oriented pairs in a field $B_0 = 0.28$ G are 316, 585, and 752 Hz. Although the number of pairs is relatively small ($\approx 9.4\%$ of the total number of Si^{29} nuclei) they can make a noticeable contribution to the resultant probability of energy absorption from the alternating field, and thus influence the form of the spectrum of the correlator $\langle I_x^2 \rangle_\nu$.

It is of interest to note that in the range from $B_0 \approx B_L$ to $B_0 \approx 2B_L$ the ratio $T_B^{-1}(2\nu_0)/T_B^{-1}(\nu_0)$ of the rates of heating via two-spin and one-spin transitions remains practically unchanged and relatively large (≈ 0.54). In the region $B_0 > 2B_L$ this ratio decreases quadratically with increase of the field (Fig. 7).
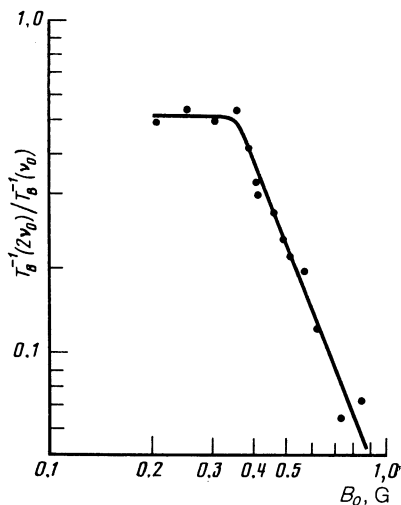

FIG. 7. Ratio of the rates of "heating" by two-spin and one-spin transitions in various fields B_0.
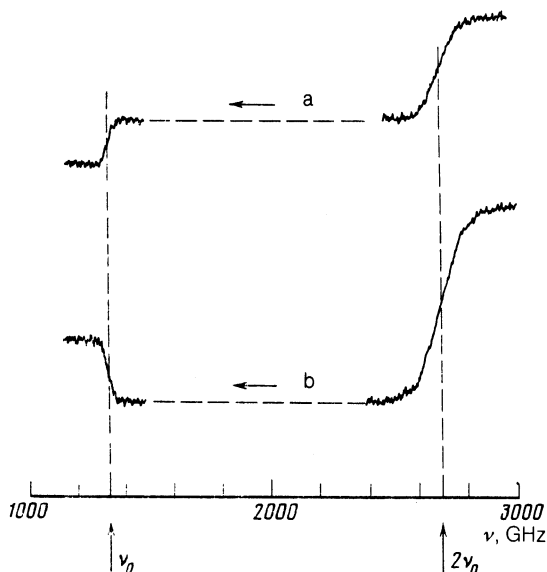
FIG. 8. Passage through two-spin resonance at $B_0 = 1.6$ G and $dv/dt = 1$ Hz/s; a) without magnetization reversal at $B_1 = 5 \cdot 10^{-3}$ G; b) with magnetization reversal at $B_1 = 2 \cdot 10^{-2}$ G.

3.5 Reversal of nuclear magnetization in two-spin resonance

The increase of the probability of forbidden transitions with decrease of the field B_0 makes it possible to observe multispin and multiphoton transitions in cases when appreciable nuclear polarization can be obtained in weak magnetic fields.

These resonances were observed earlier, for example under conditions of optical orientation of the nuclei in GaAs and GaInP crystals,[20] by the polarized luminescence method. They were also revealed by the β-decay asymmetry when Li nuclei of an LiF crystal were polarized in a nuclear reaction.[21] The theory of these resonances was considered in Refs. 22 and 23.

We present here the results of what is apparently the first observation of two-spin resonance under spin-locking conditions, when magnetization reversal takes place.

A section of the Si[29] NMR spectrum, obtained with a SQUID under fast (in the T_1 time scale) passage conditions, is shown in Fig. 8. The spectrum in Fig. 8a was obtained for $B_0 = 1.6$ G and $B_1 = 5 \cdot 10^{-3}$ G, while that in Fig. 8b was obtained for $B_0 = 1.6$ G and $B_1 = 2 \cdot 10^{-2}$ G ($dv/dt - 1$ Hz/ s). In either case, the passage was from the higher frequency. It can be seen from figure that at $B_1 = 2 \cdot 10^{-2}$ G (Fig. 8b) the passage of the two-spin resonance is accompanied by spin locking and by reversal of the magnetization, as is clearly revealed by the reversal the sign of the signal in the succeeding passage through the one-spin resonance. It is thus possible to reverse an appreciable fraction of the total magnetization by pairwise coherent motion of the nuclear spins. At $B = 5 \cdot 10^{-3}$ G (Fig. 8a) the amplitude of the alternating field is insufficient for spin locking in passage through two-spin resonance.

It must be pointed out that the nuclear magnetization is

"captured" by the effective field in the rotating coordinate frame even in passage through two-spin resonance with violation of the adiabaticity condition, which is a natural generalization of (1) to the case of a forbidden transition:

$$2\pi \, (dv/dt) \ll F(\gamma B_1)^2, \tag{14}$$

where F is the hindrance factor. The value of F for two-spin transitions in cubic crystals is $C(B_L/B_0)^2$, where C is a factor that ranges (depending on the orientation of the field B_0) from 0.76 to 1 (Ref. 20). Under the condition of the spectrum of Fig. 8a we have $F(\gamma B_1/2\pi)^2 \lesssim 0.25$.

To achieve adiabatic fast passage through spin resonance under conditions satisfying inequality (12), the field B_0 and the factor F must be increased. The first calls for better shielding of the SQUID receiving circuit, while an increase of F by lowering B_0 distorts the results because of the influence of the already considered relaxation in an alternating field ("heating" of the nuclear spin system).

It should be noted that a much lower loss of M_z on reversal of the magnetization can be obtained by measuring v in a narrower band about $2v_0$. It becomes possible then to effect repeated reversal of the magnetization in successive passages through two-spin resonance, with a loss $\delta M_z \approx 30\%$ in each reversal.

CONCLUSION

A high photonuclear magnetic susceptibility permits investigation of spin-spin interaction in a magnetically dilute system of silicon nuclei. Standard NMR technique permits observation of the undistorted width of the resonance line and of the effects of paired correlations.

The use of a SQUID extends substantially the possibilities of investigating photonuclear magnetism, and facilitates the study of the dynamics of a nuclear spin system and of its various resonant responses in weak magnetic fields.

APPENDIX

The magnetic flux passing from a sample through an annular coupling loop of radius a is

$$\Phi_0 = M \int (\mathbf{Bm}) \, dS = M \int dV \oint_l \frac{[\mathbf{mR}]}{R^3} [\mathbf{mn}] a \, d\varphi$$

$$= -Ma \int dV \frac{\mathbf{Rn}(\varphi)}{R^3} d\varphi, \tag{A.1}$$

where M is the magnetic moment per unit volume, m is a unit vector along M, n is a unit vector along the radius of the coupling loop and specifies the position of a point on the turn, R is the radius vector connecting this point with some point of the sample, and φ specifies the orientation of the vector n in the plane of the coupling turn. The integration is over the area (S) of the coupling turn, over the sample volume (V), and along the contour (l) of the coupling turn.

Recognizing that $\mathbf{R \cdot n}/R^3 = -\mathrm{div}(\mathbf{n}/R)$, we obtain for

a cylindrical sample coaxial with the coupling loop and having a radius r_0 and a length L

$$\Phi_0 = \xi_0 4\pi M, \qquad \xi_0 = \frac{L(ar_0)^{1/2}}{2^{3/2}} \int_0^\pi \frac{\sin^2 \varphi \, d\varphi}{(D - \cos \varphi)(G - \cos \varphi)^{1/2}} ,$$
(A.2)

where

$$D = (a^2 + r_0^2)/2ar_0, \qquad G = [(L/2)^2 + r_0^2 + a^2]/2ar_0.$$

A similar expression for the flux Φ_k produced by a calibrating current-carrying loop of radius r_k can be obtained by putting in (A.2) $D = G$, replacing r_0 by r_k, and substituting for $\pi r_k^2 LM$ the magnetic moment M_k of the current in the calibrating loop.

[1]M. I. D'yakonov and V. I. Perel', Zh. Eksp. Teor. Fiz. **68**, 1514 (1975) [Sov. Phys. JETP **41**, 759 (1975)].

[2]V. A. Novikov and V. G. Fleisher, *ibid.* **71**, 410 (1976) [**14**, 410 (1976)].

[3]D. Paget, G. Lampel, B. Sapoval, and V. I. Safarov, Phys. Rev. **B15**, 5780, 1977.

[4]Optical Orientation, Modern Problems in Condensed Matter Sciences, F. Meier and B. Zakharchenya, eds., North Holland, N. Y., Vol. 8, Chaps. 5 and 9.

[5]M. I. D'yakonov, V. I. Perel', V. L. Berkovits, and V. I. Safarov, Zh. Eksp. Teor. Fiz. **67**, 1912 (1974) [Sov. Phys. JETP **40**, 950 (1975)].

[6]V. P. Zakharchenya, V. K. Kalevich, V. D. Kul'kov, and V. G. Fleisher, Fiz. Tverd. Tela (Leningrad) **23**, 1387 (1981) [Sov. Phys. Solid State **23**, 810 (1981)].

[7]G. Lampel, Phys. Rev. Lett. **20**, 491 (1968).

[8]N. T. Bagarev and L. S. Vlasenko, Zh. Eksp. Teor. Fiz. **75**, 1743 (1978) [Sov. Phys. JETP **48**, 878 (1978)].

[9]L. S. Vlasenko, Izv. AN SSSR ser. fiz. **47**, 2325 (1983).

[10]L. S. Vlasenko, N. V. Zavaritskiĭ, and V. G. Fleĭsher, Pis'ma Zh. Tekh. Fiz. **9**, 1377 (1983) [Sov. Tech. Phys. Lett. **9**, 592 (1983)].

[11]I. A. Merkulov, Zh. Eksp. Teor. Fiz. **82**, 315 (1982) [Sov. Phys. JETP **55**, 188 (1982)].

[12]L. S. Vlasenko, Izv. AN SSSR ser. fiz. **46**, 469 (1982). Physica (Utrecht) 116(B), 281 (1983).

[13]N. V. Zavaritskii and A. N. Vetchinkin, Prib. Tekh. Eksp. No. 1, 207 (1974).

[14]F. S. Dzheparov and É. B. Fel'dman, Izv. AN SSSR ser. fiz. **50**, 270 (1986).

[15]A. Abragam, *The Principles of Nuclear Magnetism*, Oxford, 1961.

[16]M. Goldman, *Spin Temperature and Nuclear Magnetic Resonance in Solids*, Oxford, 1970, Chaps. 2 and 3.

[17]L. S. Vlasenko, M. P. Vlasenko, and V. M. Rozhkov, Opt. Spektr. **52**, 942 (1982).

[18]P. Sapoval and D. Lepine, J. Phys. Chem. Sol. **27**, 115 (1966).

[19]I. A. Merkulov, Zh. Eksp. Teor. Fiz. **79**, 1036 (1980) [Sov. Phys. JETP **52**, 526 (1980)].

[20]V. K. Kalevich, V. D. Kul'kov, I. A. Merkulov, and V. G. Fleĭsher, Fiz. Tverd. Tela (Leningrad) **24**, 2098 (1982) [Sov. Phys. Solid State 24, 1195 (1982)].

[21]Yu. G. Abov, M. I. Bulgakov, A. D. Gul'ko, et al., Pis'ma Zh. Eksp. Teor. Fiz. **35**, 344 (1982) [JETP Lett. 35, 424 (1982)].

[22]F. S. Dzheparov and S. V. Stepanov, Preprint ITEF-139, 1982.

[23]T. Sh. Abesadze, L. L. Buishvili, M. G. Menabde, and Z. G. Rostomashvili, Microwave Spectroscopy [in Russian], Perm' University Press, 1985, p. 99.

Translated by J. G. Adashko